Formation of excited states in high–Z helium–like systems

S. Fritzsche[a], Th. Stöhlker[b,c], O. Brinzanescu[c,d], and B. Fricke[a]

[a] *II. Fachbereich Physik, Universität Kassel, Heinrich–Plett–Str. 40, D–34132 Kassel, Germany*
[b] *Institut für Kernphysik, Universität Frankfurt, D–60486 Frankfurt, Germany*
[c] *Gesellschaft für Schwerionenforschung, Planckstraße 1, D–62491 Darmstadt*
[d] *National Institute for Laser, Plasma and Radiation Physics, RO–76900 Bucharest-Magurele, Romania*

Abstract. High–Z helium–like ions represent the simplest multi–electron systems for studying the interplay between electron–electron correlations, relativistic as well as quantum electrodynamical effects in strong fields. In contrast to the adjacent lithium–like ions, however, almost no experimental information is available about the excited states in the high–Z domain of the helium sequence. Here, we present a theoretical analysis of the x–ray production and decay dynamics of the excited states in helium–like uranium. Emphasize has been paid particularly to the formation of the $^3P_0$ and $^3P_2$ levels by using electron capture into hydrogen–like U^{91+}. Both states are of interest for precise measurements on high–Z helium–like ions in the future.

I INTRODUCTION

Up to now, very little is known about the fine structure and properties of high–Z helium–like ions. At the first glance, this is certainly surprising since these ions belong to the simplest atomic systems. While a large number of precise measurements have been carried out for the adjacent hydrogen– and lithium–like ions (see [1,2] for references), neither the fine structure nor excitation cross sections nor line intensities are accurately known for highly–charged ions in the helium sequence. Till now, precise measurements in this isoelectronic sequence were limited to rather low charge states with, say, $Z \leq 36$. For higher Z, the individual K_α and K_β transitions have not been resolved in previous experiments [3]. — Thus, despite of the apparent simplicity of helium–like ions, no reliable experimental data are in fact available for most of their excited levels in the high–Z range. So far, just a single experiment on the Lamb–shift in helium–like uranium has been carried out by Munger and Gould [4] in which a lifetime measurement of the $^3P_0$ level has been exploited in order to derive the $^3P_0 - ^3S_1$ fine structure splitting. ¿From a lifetime of 54.4 ± 3.4 ps, they obtained a $^3P_0 - ^3S_1$ transition energy of 260.0 eV with a precision of about 8 eV and, thus, could receive at least a first clue about QED contributions for helium–like uranium. Due to a relative uncertainty of about 7 %, however, all details concerning the fine–structure of these ions still remains rather uncertain.

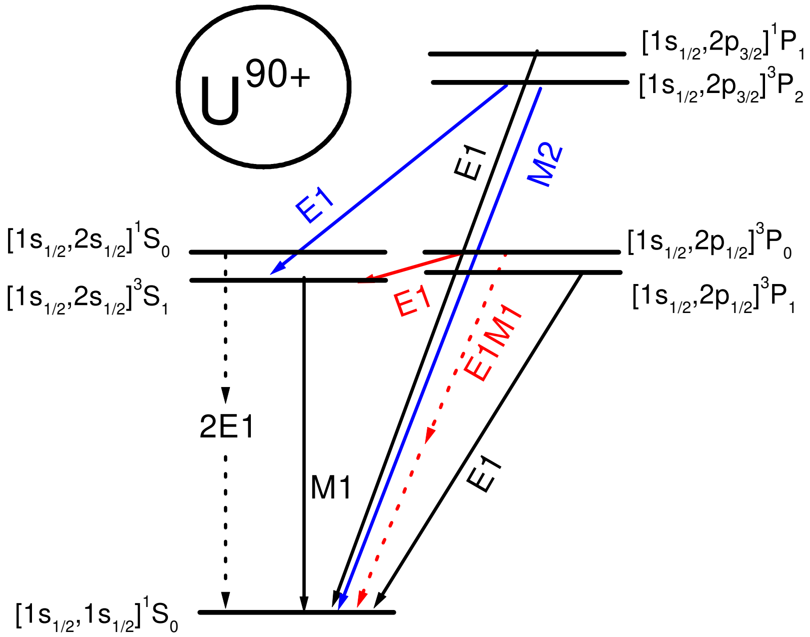

FIGURE 1. Schematic level structure and decay branches for the $n = 2$ levels of high–Z helium–like ions. The $^3P_0$ states decay either via an 253 eV $E1$ or $E1M1$ transitions with decay rates of $1.2 \cdot 10^{10}$ sec^{-1} and $5.6 \cdot 10^9$ sec^{-1}, respectively. The $^3P_2$ states decay via a 4510 eV $E1$ transition into $^3S_1$ or $M2$ transition into the ground state with decay rates of $8.6 \cdot 10^{13}$ sec^{-1} and $2.1 \cdot 10^{14}$ sec^{-1}.

For high–Z ions in the helium sequence, the $\Delta n = 0$ transitions in the $L-$shell are of particular interest because they are affected not only by the (relativistic) interaction among the electrons but also by rather strong quantum electrodynamical (QED) effects. These transitions, therefore, provide an ideal test ground to probe our understanding of the interplay between electron–electron correlations, relativistic, as well as QED effects in many–particle systems. Fig. 1 shows the schematic level structure and decay branches for the $n = 2$ levels in high–Z ions. Two suitable candidates for QED studies are the $1s2p\ ^3P_0 - 1s2s\ ^3S_1$ ($\Delta E \approx 253\ eV$ in U^{90+}) and the $1s2p\ ^3P_2 - 1s2s\ ^3S_1$ ($\Delta E \approx 4.51\ keV$ in U^{90+}) transitions for which precise measurements are required in order to determine the level scheme in the high–Z range. Theoretical calculations on these transitions have been carried out by several groups [5–7] but lead to deviations which are of the order of a few eV, i.e. rather large if compared with the currently available precision for the excited states in high–Z hydrogen– and lithium–like ions. Although these deviations are mainly a result of the different treatment of the electron–electron interaction, a direct comparison of the individual (theoretical) contributions is often not easy and can certainly not *replace* accurate measurements of the fine structure and lifetimes for high–Z helium–like ions [8,9].

Precise energy measurements of the $\Delta n = 0$ transitions in high–Z helium–like ions have not been possible up to now due to the lack of luminosity. At the BEVALAC accelerator, for example, the low beam currents do so far not accomplish the use of crystal spectrometers with their low detection efficiency. Similarly, at the Super–EBIT device, a previous attempt [10] to measure the $1s2p\ ^3P_2 \rightarrow 1s2s\ ^3S_1$ transition energy in helium–like U^{90+} failed since the population of the $1s2p\ ^3P_2$ level by electron impact turned out to be not efficient enough. — However, an alternative access to the fine structure of helium–like ions is provided by the long living, metastable $1s2p\ ^3P_0$ level. For this level, a precise lifetime measurement would enable one not just to collect information about the fine structure splitting of the $1s2s\ ^3S_1$ and $1s2p\ ^3P_0$ levels but would also probe our knowledge of the atomic wave functions in calculating accurate transition probabilities. As seen from Fig. 1, the $1s2p\ ^3P_0$ level decays either by an E1 transition to $1s2s\ ^3S_1$ or via a two–photon E1M1 emission into the $1s^2\ ^1S_0$ ground state whereby the rates for both channels are of about the same magnitude. Hereby, a *direct* lifetime measurement of the $^3P_0$ level can be conducted by means of the $1s2s\ ^3S_1 - 1s^2\ ^1S_0$ M1 transition whose decay rate is more than four orders of magnitude faster than the precursory decay of $1s2p\ ^3P_0$ level.

In the following of this contribution, we investigate and discuss conditions to determine lifetimes for the $1s2p\ ^3P_0$ level as well as to carry out a direct energy measurement of the $1s2p\ ^3P_2 \rightarrow 1s2s\ ^3S_1$ transition in high–Z helium–like ions (like U^{90+}) by utilizing electron capture into the hydrogen–like species.

II DECAY DYNAMICS AND X–RAY PRODUCTION

To simulate the projectile x–ray production which is induced by electron capture, the two relevant capture processes are non–radiative and radiative capture. Generally, both capture processes have to be considered in order to obtain the initial population distribution at either a gaseous target or at the foil. While a continuum distorted–wave (CDW) approach has been applied to the non–radiative capture, the (nlj)–dependent cross sections for a radiative capture were calculated within the dipole–approximation (see Ref. [11]). For the cases of initially bare and helium–like uranium, these assumptions have recently lead to an excellent agreement between experimental and simulated x–ray spectra for a wide range of energies from 49 MeV/u to 350 MeV/u [11].

For the *prompt* capture of electrons inside the foil, the same approximations as for bare ions can be applied also for helium–like ions since an electron capture occur for high–Z ions predominantly into highly–excited subshells, rather independent of the additional $1s$ electron. After the capture, then, the excited ions stabilize themselve by a cascade of radiative transitions whose decay dynamic is well described by a system of rate equations

$$\frac{dN_i}{dt} = - \sum_j^{(<)} \lambda_{ij}\, N_i + \sum_k^{(>)} \lambda_{ki}\, N_k \qquad \forall\, i = 1, \ldots, \Lambda\,. \tag{1}$$

In these equations, Λ is the total number of (excited) levels which are considered in the decay cascade; the index j runs over all levels with total energy $E_j < E_i$ and

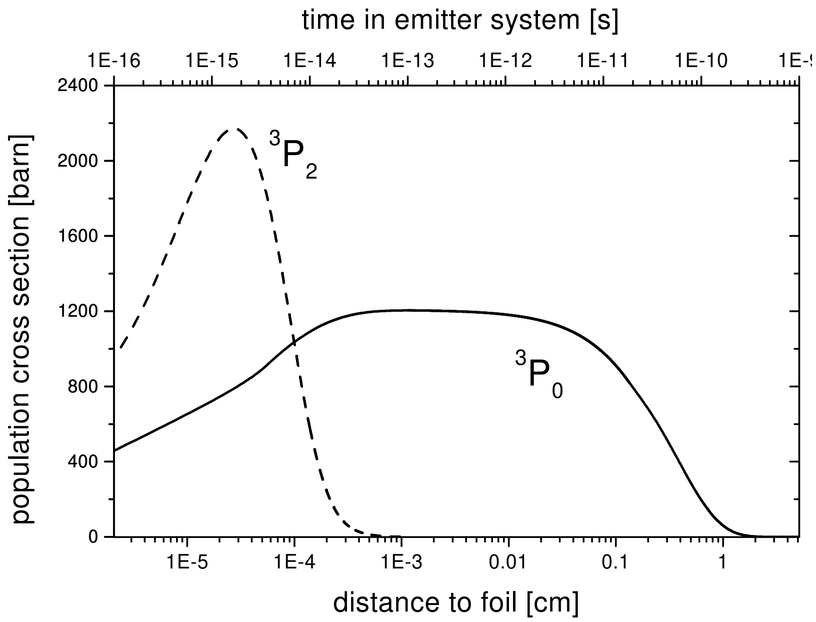

FIGURE 2. Occupation of the $^3P_0$ and the $^3P_2$ levels in helium–like uranium as a function of the time or, equivalently, their distance from the foil (compare text). An initial electron capture has been assumed for 200 MeV/u hydrogen–like ions at a foil.

k over all those with $E_k > E_i$. Apart from its (exponential) decay into lower–lying levels, each level will also be 'feeded' from levels having higher energies. In fact, most of the excited levels have a rather large number of decay branches and at least one fast E1 branch ($\approx 10^{14}$ sec^{-1}). Purely the $1s2p\ ^3P_0$ level occurs to be metastable ($\Gamma \approx 10^{10}$ sec^{-1}) for high–Z helium–like ions. For simulating the time evolution of Eq. (1) for electron capture in a foil, we assumed that states with total angular momenta $J \leq 3$ and principal quantum numbers $n \leq 9$ need to be considered because the initial capture occurs in a solid. This *cut off* concerning the angular momentum and higher subshells accounts for the large depopulation cross–sections for highly–excited states owing to the large particle density in a solid. For a rough estimation of this 'depopulation' effect one may define a decay cross–section σ_Γ given by

$$\sigma_\Gamma = \lambda \cdot [\rho \cdot \beta \cdot \gamma \cdot\ c]^{-1} \qquad (2)$$

where γ and β denotes relativistic factors, c the speed of light, ρ the target density, and λ the overall rate. This 'decay' cross–section σ_Γ has to be compared with the ionization cross–section σ_{ion} which scales approximately with n^4. To demonstrate this *solid–state* effect we consider, for example, a carbon target at 100 MeV/u and the $n = 7, l = 4$ subshell for helium–like uranium. In this case, the ratio $\sigma_{\text{ion}}/\sigma_\Gamma \approx 4$, i.e. a re–ionization is likely to occur before its radiative stabilization to some lower–lying level. The restriction $J \leq 3$ and $n \leq 9$ leads to a total of 121 excited levels which were taken into account in the time evolution of Eq. (1). For the individual decay branches, moreover, we included all multipole components of the radiation field up to the magnetic–dipole ($M2$) and electric–octupole ($E3$) modes.

This results in a total of about 5149 decay channels which have been accounted for in our present computations. Hereby, all transition energies and decay rates have been generated from (configuration–averaged) wave functions of the GRASP–92 program [12]. For optimizing the wave functions, several groups of levels have been considered together and the main relaxation effects included by applying our newly developed transition probability code [13]. For the $1s2p\ ^3P_0$ and $1s2s\ ^1S_0$ level, in addition, rather strong *two–photon* transitions occur whose rates [14] have also been incorporated into Eq. (1).

As a result of our simulation, Fig. 2 depicts the population probability of the $^3P_0$ level for helium–like uranium as function of time (t) in the emitter frame (upper x–axis). In this figure, we assumed a carbon target and a collision energy of 200 MeV/u. Moreover, the lower x–axis refers to the distance $d = \gamma \cdot \beta \cdot c \cdot t$ of the ion from the foil. Note, that at $t = 0$ the population of the $^3P_0$ level by direct capture is rather small and amounts to about $\sigma = 200$ barn (not shown in the figure). However, owing to the feeding from higher–lying levels, the population probability increases for this level by more than a factor of five and reaches a saturation after 5×10^{-13}sec. But only after about 5×10^{-10}sec, which corresponds to a distance of about 2 mm from the foil, no additional feeding of the $^3P_0$ level arises and the population of this particular level then approaches an exponential (decay) behaviour. For an energy of 200 MeV/u, consequently, distances of closer than 2 mm must be avoided in any experiment in order to guarantee a correct lifetime measurement. For comparison, we display in Fig. 2 also the time evolution of the $^3P_2$ level ($\Gamma \approx 10^{14}\text{sec}^{-1}$) which shows that at such distances all the other L–shell levels are completely depopulated.

Apart from the population of excited states by electron capture inside a foil, the use of a jet–target as available at the storage ring ESR is also of interest. Owing to its length of 5 mm, however, this target is not appropriate for a lifetime measurement; still, it may support precise experiments of the $^3P_2 -^3 S_1$ level splitting. Beside of the geometry, the main difference between the jet and a solid target concerns the particle densities. While, in a solid, the density ρ is typically of the order of 10^{23} p/cm^3, the jet–target has a density of only about 10^{12} p/cm^3. Thus, no density effects as discussed above for the excitation at a foil need to be taken into accout at the jet–target. For a jet–target, in fact, a capture of electrons has been observed even into subshells with $n \approx 20$ at the ESR [11]. In order to estimate the strength of the $^3P_2 -^3 S_1$ x–ray line for U^{90+}, we therefore carried out a spectrum simulation for the collision system $U^{91+} \rightarrow N_2$ at 100 MeV/u for which all levels up to $n = 20$ have been incorporated in the rate equations (1). Such an elaborate computation leads to a total of 435 levels and involves more than 42000 individual transition channels.

By using a jet target, we suppose that the decay of all levels occurs (more or less) instantaneously if compared with the length of the target. Apart from the $^3P_0$ level which has no influence on the time evolution of the (upper) $^3P_2$ level, this assumption has been well confirmed by our computations. In Fig. 3, the result of a simulated x–ray spectrum is depicted by assuming an experimental resolution of

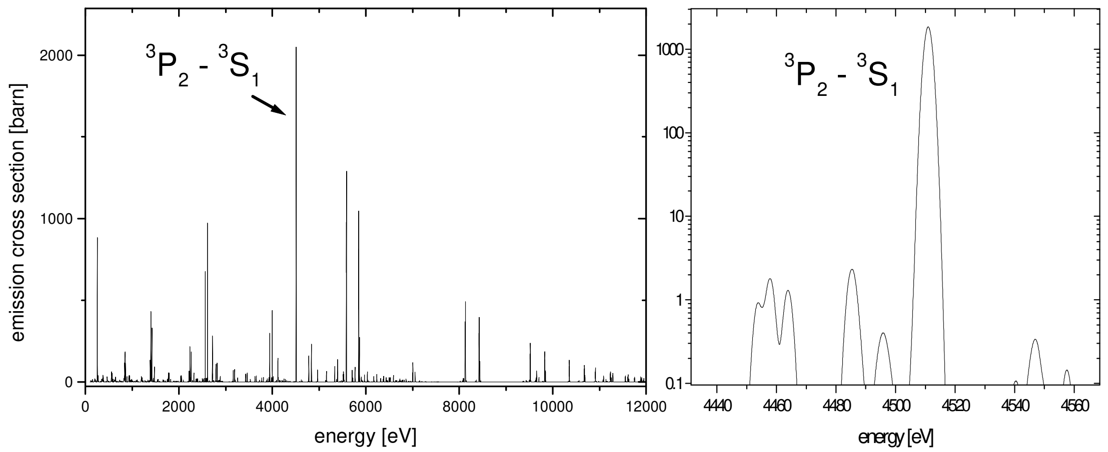

FIGURE 3. Simulated x–ray spectrum of U^{90+} ions. Here, the excited states are formed by electron capture from a N_2 jet–target in collision with U^{91+} ions at 100 MeV/u. For the calculation, excited levels up to $n = 20$ have been taken into account.

3 eV. The energy range of this theoretical spectrum covers all transitions below 13 keV, i.e. all those transitions involving the M and higher shells as well as the intra L–shell transitions. Most remarkably, the $^3P_2 -^3 S_1$ x–ray line turns out to be the most intensive transition in this energy range. Its calculated total production cross–section amounts to about 2 Kbarn. Note, moreover, that no line blends should disturb a precise measurement as could be caused by higher Rydberg transitions (compare the right part of Fig. 3).

III SUMMARY

In summary, a theoretical study of the x–ray production and decay dynamics of the excited states in helium–like uranium are discussed for the case of U^{91+} ions in collision with solid and gaseous matter. For the $^3P_0$ level, our extensive theoretical analysis allows us to understand the feeding and cascade population as function of the distance from the foil. This provides us with necessary information for a precise lifetime measurement in future experiments. Concerning the population of the $^3P_2$ level, our analysis predicts that this level can be populated very efficient at the ESR jet target — quite in contrast to a former experiment where electron–impact excitation has been applied. For this level, no line blends has been found from Rydberg transitions. Both, a precise lifetime experiment as well as energy determination of the $^3P_2 -^3 S_1$ transition will constitute a unique probe of our current understanding of the simplest multi–electron systems in the high–Z domain, a test which has been missing till today.

REFERENCES

1. H. F. Beyer and Th. Stöhlker, in print (1999).

2. P. Beiersdorfer, K. Widmann, J. Crespo Lopez–Urrutia, Hyperfine Int. 114 (1998) 141.
3. P. H. Mokler, Th. Stöhlker, C. Kozhuharov, R. Moshammer, P. Rymuza, F. Bosch, T. Kandler, Phys. Scr. T 51 (1994) 28.
4. C. T. Munger and H. Gould, Phys. Rev. Lett. 57 (1986) 2927.
5. G. W. F. Drake, Can. J. Phys. 66 (1988) 586.
6. M. H. Chen, K. T. Cheng, and W. R. Johnson, Phys. Rev. A 47 (1993) 3692.
7. D. R. Plante, W. R. Johnson, and J. Sapirstein, Phys. Rev. A 49 (1994) 3519.
8. R. E. Marrs, S. R. Elliott, and Th. Stöhlker, Phys. Rev. A 52 (1995) 3577.
9. Th. Stöhlker and E. A. Livingston, Acta Phys. Pol. 27 (1996) 441.
10. P. Beiersdorfer, S. R. Elliott, A. Österheld, Th. Stöhlker, J. Autrey, G. Brown, A. J. Smith, and K. Widmann, Phys. Rev. A 53 (1996) 4000.
11. Th. Stöhlker, Phys. Scr. T 80 (1999) 165.
12. F. A. Parpia, C. Froese Fischer and I. P. Grant, Comp. Phys. Commun. 94 (1996) 249.
13. S. Fritzsche, C. Froese Fischer, and C. Z. Dong, Comp. Phys. Commun. in print (1999).
14. G. W. F. Drake, Phys. Rev. A 34 (1986) 2871.